

**Sr<sub>2</sub>VO<sub>4</sub> and Ba<sub>2</sub>VO<sub>4</sub> under pressure: An orbital switch and potential *d*<sup>1</sup> superconductor**R. Arita,<sup>1</sup> A. Yamasaki,<sup>2,\*</sup> K. Held,<sup>2</sup> J. Matsuno,<sup>1</sup> and K. Kuroki<sup>3</sup><sup>1</sup>RIKEN, Wako, Saitama 351-0198, Japan<sup>2</sup>Max-Planck-Institut für Festkörperforschung, 70569 Stuttgart, Germany<sup>3</sup>Department of Applied Physics and Chemistry, University of Electro-Communications, 1-5-1 Chofugaoka, Chofu-shi, Tokyo 182-8585, Japan

(Received 15 February 2007; published 23 May 2007)

We study Sr<sub>2</sub>VO<sub>4</sub> and Ba<sub>2</sub>VO<sub>4</sub> under high pressure by means of the local-density approximation + dynamical mean-field theory method. While Sr<sub>2</sub>VO<sub>4</sub> is a 1/6-filling three-band system at ambient pressure with a small level splitting between the  $d_{xy}$  and  $d_{yz/zx}$  bands, we show that an orbital polarization occurs under uniaxial pressure, which will lead to dramatic changes of the magnetic and transport properties. When pressure is applied in the *c* direction, a *d*<sup>1</sup> analog of *d*<sup>9</sup> cuprates is realized, making Sr<sub>2</sub>VO<sub>4</sub> a possible candidate for a *d*<sup>1</sup> superconductor. We also study the effect of chemical pressure by substituting Sr by Ba, and find that a *d*<sup>1</sup> analog of cuprates can be realized more easily by growing Ba<sub>2</sub>VO<sub>4</sub> on a substrate with lattice constant of 4.1–4.2 Å.

DOI: [10.1103/PhysRevB.75.174521](https://doi.org/10.1103/PhysRevB.75.174521)

PACS number(s): 71.27.+a, 71.30.+h

**I. INTRODUCTION**

Since the discovery of high-temperature superconductivity in cuprates,<sup>1</sup> strongly correlated electron systems (SCESs) and their intriguing magnetic, dielectric, optical, and transport properties have been at the center of solid-state research. Hence, a quantitative reliable calculation of correlation effects from first principles is one of the most important challenges. This is particularly difficult since the standard local-density approximation (LDA) in the framework of density-functional theory<sup>2</sup> fails if electronic correlations are strong. Recently, however, a variety of attempts which go beyond LDA have been undertaken, and many successes have been achieved.<sup>3</sup>

The next step in this direction is the (theoretical) materials design of SCES with specific properties and the simulations of SCES under extreme conditions. As a touchstone for such attempts, we study the electronic structure of Sr<sub>2</sub>VO<sub>4</sub> and Ba<sub>2</sub>VO<sub>4</sub> under high pressure by means of the LDA + dynamical mean-field theory (DMFT) method,<sup>4</sup> one of the most widely used approaches for realistic calculations of SCES.<sup>5</sup>

The reason why we focus on Sr<sub>2</sub>VO<sub>4</sub> is twofold. First, Sr<sub>2</sub>VO<sub>4</sub> is a layered perovskite, as cuprates and ruthenates<sup>6</sup> which show unconventional superconductivity. Second, the challenge to synthesize single-crystalline Sr<sub>2</sub>VO<sub>4</sub> has been overcome quite recently: Matsuno *et al.*<sup>7</sup> employed epitaxial growth techniques for growing a thin Sr<sub>2</sub>VO<sub>4</sub> film. Hence, a detailed investigation of the electronic structure becomes now possible.

As for the first point, in fact, Sr<sub>2</sub>VO<sub>4</sub> attracted attention because it is a “dual” material of La<sub>2</sub>CuO<sub>4</sub>. Namely, the former has one 3*d* electron per V site (*d*<sup>1</sup> system), while the latter has nine 3*d* electrons per Cu site (*d*<sup>9</sup> system). However, as was already pointed out by Pickett *et al.* in 1989,<sup>8</sup> there is a big difference between these oxides. While La<sub>2</sub>CuO<sub>4</sub> is a 1/2-filling single-band ( $d_{x^2-y^2}$ ) system, Sr<sub>2</sub>VO<sub>4</sub> is a 1/6-filling three-band ( $d_{xy}/d_{yz/zx}$ ) system, since the level splitting of  $t_{2g}$  in the latter material is much smaller than that of

$e_g$  in the former. Therefore, the theoretical idea of unconventional superconductivity in Sr<sub>2</sub>VO<sub>4</sub> has been dismissed.

Also experimentally, Sr<sub>2</sub>VO<sub>4</sub> and La<sub>2</sub>CuO<sub>4</sub> behave indeed differently. Magnetic properties and transport properties were measured for a polycrystal of Sr<sub>2</sub>VO<sub>4</sub> in the early 1990s,<sup>9</sup> indicating that Sr<sub>2</sub>VO<sub>4</sub> is an antiferromagnetic insulator (semiconductor) with a low Néel temperature  $T_N \sim 45$  K. However, in contrast to La<sub>2</sub>CuO<sub>4</sub>, a small ferromagnetic moment was also observed. In recent measurement of the optical conductivity for a single-crystalline thin film, a small gap structure, i.e., a peak around 1 eV and a shoulder around 0.5 eV, was observed.<sup>7</sup>

Theoretically, several first-principles calculations beyond LDA were performed, and it was confirmed that the relation between Sr<sub>2</sub>VO<sub>4</sub> and La<sub>2</sub>CuO<sub>4</sub> is not dual.<sup>10,11</sup> Specifically, Imai *et al.* carried out an LDA + path-integral renormalization group calculation and found a nontrivial orbital-stripe order.<sup>10</sup> These orbital degrees of freedom are irrelevant in cuprates.

The motivation of the present study is based on the following idea: While Sr<sub>2</sub>VO<sub>4</sub> and La<sub>2</sub>CuO<sub>4</sub> are certainly not dual at ambient pressure, we hope to change this by changing the atomic configuration of the octahedron around the V ion. Here, we consider the application of high uniaxial pressure, synthesize films on substrates with appropriate lattice constant, and introduce chemical pressure (substitute Sr by Ba). If the level splitting between the  $d_{xy}$  and  $d_{yz/zx}$  orbitals becomes larger, it will lead to an orbital polarization, so that the system might actually become a *d*<sup>1</sup> analog of *d*<sup>9</sup> cuprates. In this paper, we examine this idea by means of LDA + DMFT.<sup>12</sup>

**II. GGA OPTIMIZATION OF CRYSTAL STRUCTURE**

Let us now turn to our actual calculations. First, we perform a generalized gradient approximation (GGA) calculation with plane-wave basis, employing the Tokyo *ab initio* program package (TAPP).<sup>13</sup> Note that a plane-wave basis set

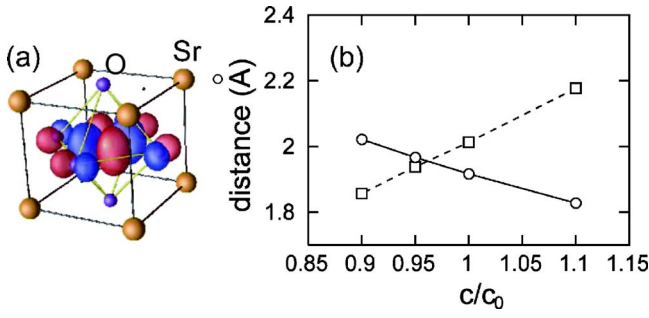


FIG. 1. (Color online) (a) NMTO Wannier function of the V  $d_{xy}$  orbital for  $\text{Sr}_2\text{VO}_4$ , shown together with the oxygen and Sr ions. The position of Sr and the apical oxygen are optimized by a plane-wave GGA calculation. (b) GGA-optimized distance between O and V along the  $c$  direction (open squares) and in the  $ab$  plane (open circles) as a function of the  $c$ -axis elongation  $c/c_0$ .

has advantages for optimizing atomic configurations under high pressure which are unknown experimentally. We adopt the exchange-correlation functional introduced by Perdew *et al.*<sup>14</sup> and ultrasoft pseudopotentials in a separable form.<sup>15,16</sup> The wave functions are expanded up to a cut-off energy of 36.0 Ry. We assume that the system has the same  $I4/mmm$  symmetry as the experimental one at atmospheric pressure,<sup>17</sup> so that there are only two free parameters, i.e., the position of the apical oxygen and Sr. In Fig. 1(a), we show the atomic configuration of the octahedron around the V ion. The convergence criterion of the geometry optimization is that all forces acting on atoms in the system become smaller than  $2 \times 10^{-3}$  hartree/a.u., and we obtain the same optimized configuration for  $8 \times 8 \times 8$ ,  $12 \times 12 \times 12$ , and  $12 \times 12 \times 4$   $k$ -point grids.

We calculate the total energy as a function of the lattice constant  $a$ , fixing the ratio  $c/a$  to its experimental value ( $\approx 3.28$ ).<sup>9</sup> We find that the energy minimum is at  $a = 3.89$  Å (not shown), in excellent agreement with experiment ( $a = 3.84$  Å). When the lattice constant  $a$  is fixed to this optimized value, the Sr-V and O-V distances along the  $c$  direction become 4.46 and 2.01 Å, respectively, consistent with the experimental values of 4.46 and 1.98 Å.

Next, we change the lattice constants to simulate the effect of pressure. Considering the application of high uniaxial pressure or, more realistically, the synthesis of  $\text{Sr}_2\text{VO}_4$  films on substrates with appropriate lattice constant, we change the lattice constant  $c$  up to  $\pm 10\%$  of the experimental value  $c_0 = 12.6$  Å.

In Fig. 1(b), we plot the GGA-optimized distance between O and V along the  $c$  direction ( $d_c$ ) and within the  $ab$  plane ( $d_{ab}$ ) as a function of  $c/c_0$ . Here, we fix the volume of the unit cell ( $V$ ) rather than  $a$ , since the total energy at fixed  $V$  is always lower than that of fixed  $a$ . While the V-O distance  $d_c$  is longer than  $d_{ab}$  at ambient pressure,  $d_c$  becomes shorter than  $d_{ab}$  for  $c/c_0 < 0.95$ .

In fact, the ratio  $d_c/d_{ab}$  determines the splitting of the three  $t_{2g}$  orbitals. If we press uniaxially along the  $c$  direction, the negatively charged oxygen ions move toward the vanadium site. Hence, the energy of the  $d_{yz/zx}$  orbitals, which point along the  $c$  direction, is enhanced. At ambient pressure, the level splitting is small. However, given the fact that  $d_c$

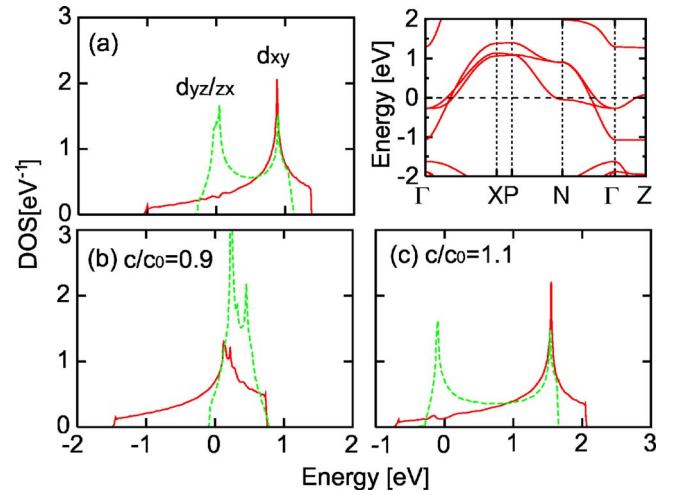


FIG. 2. (Color online) Density of states of the  $t_{2g}$  band obtained by LDA calculation for (a) atmospheric pressure, (b) uniaxial pressure in the  $c$  direction ( $c/c_0 = 0.9$ ), and (c) uniaxial pressure in the  $ab$  plane ( $c/c_0 = 1.1$ ). The solid (dashed) line is for the  $d_{xy}$  orbital ( $d_{yz/zx}$  orbitals). Inset: LMTO band structure for atmospheric pressure.

and  $d_{ab}$  change considerably with  $c/c_0$  in Fig. 1(b), we may expect that we can control the level splitting and, consequently, the orbital occupation by applying pressure.

### III. LDA+DMFT CALCULATION

To examine this idea in the presence of electron correlations, we perform LDA+DMFT calculations for the atomic configurations obtained above. To this end, we first carry out LDA band-structure calculations with the linearized muffin-tin orbital (LMTO) basis.<sup>18</sup> In the inset of Fig. 2, we show the obtained band structure for ambient pressure. Almost the same band structure is obtained by the GGA calculation with plane-wave basis.

Then, we extract the three  $t_{2g}$  bands by the  $N$ th-order muffin-tin orbital (NMTO) downfolding<sup>19</sup> using the generated LDA potential. As a typical example of the resulting NMTO Wannier functions, we show the  $d_{xy}$  orbital of V in Fig. 1(a) for ambient pressure. The densities of states of the  $t_{2g}$  band for  $c/c_0 = 0.9$ , 1.0, and 1.1 are shown in Fig. 2. The NMTO bandwidth of the  $d_{xy}$  band is 2.46 eV at ambient pressure ( $c = c_0$ ). This value is consistent with that of the GGA calculation with plane-wave basis and that of Pickett *et al.* who used the full-potential linearized augmented plane wave basis.<sup>8</sup> Imai *et al.*<sup>10</sup> reported a smaller bandwidth of  $\sim 2.0$  eV.<sup>20</sup>

For the case of  $c/c_0 = 0.9$  (1.1), Fig. 2 shows that the center of gravity of the  $d_{yz/zx}$  bands is clearly higher (lower) than that of the  $d_{xy}$  band. Indeed, as we can see in Fig. 3(a), the crystal-field splitting between the  $d_{xy}$  and  $d_{xz/yz}$  orbitals in the NMTO Hamiltonian is  $-382$  ( $+434$ ) meV for  $c/c_0 = 0.9$  (1.1). Concerning the electron occupation of the  $d_{xy}$  and  $d_{xz/yz}$  orbitals, 90% (20%) of the  $d$  electrons are accommodated in the  $d_{xy}$  band for  $c/c_0 = 0.9$  (1.1), in contrast to ambient pressure where all three  $t_{2g}$  bands are similarly occupied [Fig. 3(b)].

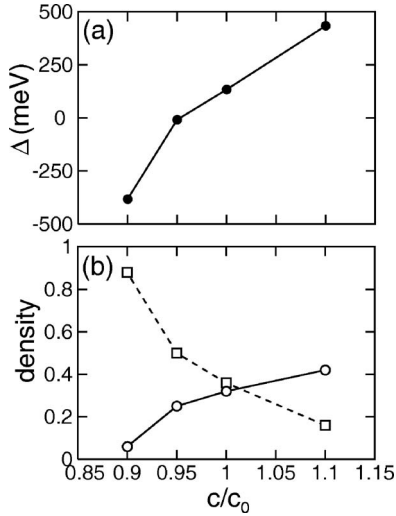


FIG. 3. (a) NMTO crystal-field splitting between the  $d_{xy}$  and  $d_{xz/yx}$  orbitals. (b) Electron occupations for the  $d_{xy}$  (squares) and  $d_{xz/yx}$  orbitals (circles).

Next, we perform DMFT calculations for the three low-energy  $t_{2g}$  bands, studying whether electronic correlations result in a full orbital polarization for  $c/c_0=0.9$  and 1.1. To this end, the DMFT effective impurity model is solved by the standard Hirsch-Fye quantum Monte Carlo (QMC) method,<sup>21</sup> where the temperature is 0.1 eV with 100 imaginary time slices and the number of QMC sample is  $\sim 2 \times 10^6$ . We employ the relation  $U=U'+2J$  where  $U$ ,  $U'$ , and  $J$  are the intraorbital Coulomb interaction, the interorbital Coulomb interaction, and the Hund coupling, respectively.

We first calculate the spectral function for ambient pressure with various interaction parameters  $U'$ , fixing  $J=0.7$  eV which is a reasonable value for V ions. In Fig. 4, we show the spectral function for  $U'=2.5$  eV (a) and 2.8 eV [(b) and (c)]; the Mott-Hubbard transition occurs around

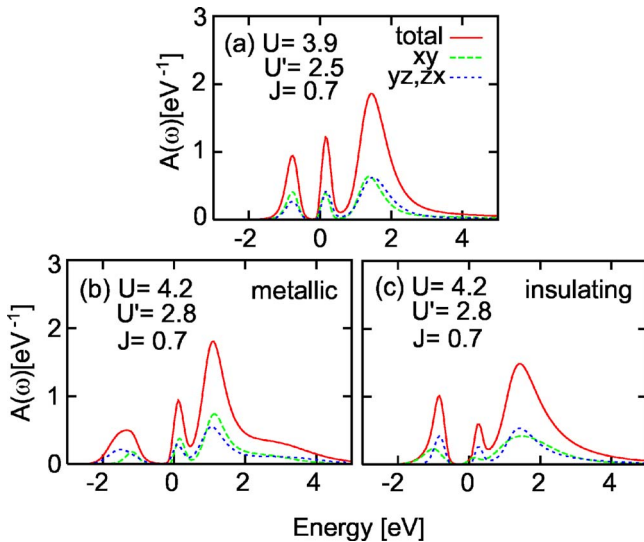


FIG. 4. (Color online) LDA+DMFT spectral function for atmospheric pressure, where the dashed, dotted, and solid lines are for  $d_{xy}$ ,  $d_{xz/yx}$ , and the total Sr<sub>2</sub>VO<sub>4</sub> spectrum, respectively. For  $U'=2.8$  eV, two solutions [(b) metallic and (c) insulating] coexist.

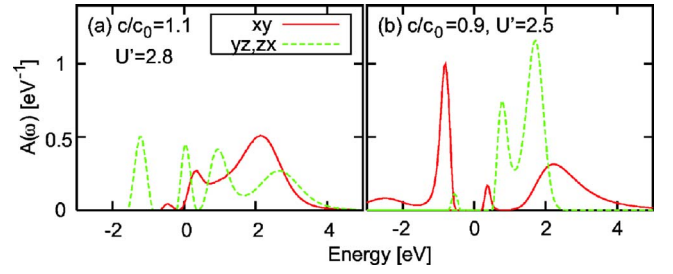


FIG. 5. (Color online) Same as Fig. 4 but for (a) uniaxial pressure in the  $ab$  plane ( $c/c_0=1.1$ ) with  $U'=2.8$  eV and (b) uniaxial pressure in the  $c$  direction ( $c/c_0=0.9$ ) with  $U'=2.5$  eV.

$U'=2.5$ – $2.8$  eV. Since the gap in (c) is in accord with the main optical peak in experiment,<sup>7</sup> we expect  $U' \sim 2.8$  eV for Sr<sub>2</sub>VO<sub>4</sub>. The coexistence of this insulating solution (c) with a metallic one (b) indicates insulating Sr<sub>2</sub>VO<sub>4</sub> to be close to a Mott-Hubbard transition.

Note that Imai *et al.*<sup>10</sup> estimated smaller Coulomb interactions:  $U' \sim 1.3$  eV and  $J \sim 0.65$  eV by the combination of the constrained LDA and the GW method.<sup>10</sup> However, as mentioned above, the bandwidth of the  $t_{2g}$  orbitals of Ref. 10 is 20%–25% smaller than that of the present study. If we normalize the interaction parameters by the bandwidth, the difference is not so big. On the other hand, Sekiyama *et al.* employed  $U'=3.55$  eV and  $J=1.0$  eV in their LDA+DMFT calculation for Sr<sub>2</sub>VO<sub>3</sub>, reproducing the photoemission spectrum of Sr<sub>2</sub>VO<sub>3</sub>.<sup>22</sup> These values are not so far from ours.

Let us now turn to the LDA+DMFT results for high pressure. In Fig. 5(a), we plot the spectral function for  $c/c_0=1.1$ , showing a metallic peak at the Fermi level. In contrast to ambient pressure, there is no coexisting insulating solution at  $c/c_0=1.1$ , i.e., applying pressure in the  $ab$  plane makes Sr<sub>2</sub>VO<sub>4</sub> metallic. An important point is that the  $d_{xy}$  orbital is almost empty for  $c/c_0=1.1$ : orbital polarization occurs. The system becomes a quarter-filled two-band Hubbard model which is well known to have a ferromagnetic ground state.<sup>23,24</sup> Therefore, we expect ferromagnetic spin fluctuation to be dominant at low  $T$  if pressure is applied in the  $ab$  plane.

On the other hand, Fig. 5(b) shows the result for uniaxial pressure along the  $c$  direction ( $c/c_0=0.9$ ). We see that the spectrum is now clearly insulating, even for the smaller value of  $U'=2.5$  eV for which we have a metal in Fig. 4(a). This is interesting since applying pressure usually makes an insulator metallic, not a metal insulating as from Figs. 4(a) and 5(b). This behavior can be understood as follows. From Fig. 2, we see that the LDA bandwidth does not change strongly from 2.26 eV at  $c/c_0=1$  to 2.46 eV at  $c/c_0=0.9$ . This small change of bandwidth alone would indeed indicate more metallic behavior, as usual. However, more important is that uniaxial pressure changes the crystal-field splitting: The two  $d_{yz/zx}$  orbitals become unoccupied, and then the large intraorbital repulsion  $U$  makes the remaining (single)  $d_{xy}$  orbital Mott insulating. This way, a  $d^1$  analog of  $d^9$  cuprates is realized. Concerning the magnetic properties, contrary to the case where the pressure is applied within the  $ab$  plane, we expect an antiferromagnetic instability, since the



system becomes a half-filled single-band model. Let us note that we did not study this antiferromagnetic phase. To this end, DMFT calculations in a symmetry-broken phase or beyond DMFT (Ref. 25) methods would be necessary.

Lastly, let us look at the energy scale of the NMTO effective Hamiltonian. We find that the nearest-neighbor hopping  $t$  is 0.26 eV and the next-nearest-neighbor hopping  $t'$  is 0.06 eV. It is interesting to compare these values with the parameters for the effective single-band Hubbard model for cuprates:  $t=0.4$  eV,  $t'=-0.07$  eV, and  $U=5$  eV.<sup>26</sup> While the possibility of superconductivity should be examined explicitly, this comparison indicates that  $\text{Sr}_2\text{VO}_4$  under high uniaxial pressure is a potential candidate for unconventional superconductivity.

#### IV. EFFECT OF CHEMICAL PRESSURE

While it is an interesting possibility to change the electronic properties by controlling the lattice constant, it might be difficult to change its value up to  $\pm 10\%$ . For example, in order to grow  $\text{Sr}_2\text{VO}_4$  thin films with  $c/c_0=0.9$ , we need a considerably large lattice mismatch between a substrate and bulk  $\text{Sr}_2\text{VO}_4$ . Such an excessive mismatch often results in lattice relaxation.

Thus, lastly, we consider the possibility of chemical pressure by substituting Sr by Ba. Since the ion radius of Ba is larger than that of Sr, the crystal is expected to be expanded. The important point here is that the V-O distance in the  $ab$  plane and that along the  $c$  axis will increase differently. Namely, while the increase of  $a$  directly affects the V-O distance in the  $ab$  plane (the latter is exactly half of the former),  $c$  and the V-O distance along the  $c$  axis are independent parameters.

First, we perform GGA calculation with structure optimization for  $\text{Ba}_2\text{VO}_4$  by changing  $a$  and  $c$ . The energy minimum is at  $a=4.04$  Å and  $c/a=3.36$ , and the V-O distances are 2.02 Å in the  $ab$  plane (compared to 1.92 Å for  $\text{Sr}_2\text{VO}_4$ ) and 2.01 Å along the  $c$  direction (2.01 Å for  $\text{Sr}_2\text{VO}_4$ ). This means that the situation for  $\text{Ba}_2\text{VO}_4$  is similar to that of  $\text{Sr}_2\text{VO}_4$  with  $c/c_0=0.95$ , i.e., if uniaxial pressure is already applied.

Next, we consider the compression  $c/c_0=0.95$  for  $\text{Ba}_2\text{VO}_4$ . The orbital polarization becomes larger, i.e., the electron density is 0.73 for the  $d_{xy}$  band and 0.14 for the  $d_{yz/zx}$  band. Thus, it is interesting to proceed with DMFT calculations. In Fig. 6, we plot the resulting LDA+DMFT spectral function for ambient pressure and uniaxial pressure in the  $c$  direction ( $c/c_0=0.95$ ) with  $U'=2.5$  eV, along with the density of states by LDA. We can see that a large orbital polarization is realized even for  $c/c_0=0.95$ . Since the relative hopping and interaction parameters for the  $d_{xy}$  band are very similar to those of the cuprates, a  $d^1$  analog of  $d^9$  cuprates can be realized. Experimentally, the uniaxial pressure is best realized by growing  $\text{Ba}_2\text{VO}_4$  on a substrate with a larger in-plane lattice constant of 4.1–4.2 Å. Such a lattice mismatch of  $\sim 5\%$  is at the edge of what is doable experimentally since it results in a strong elastic strain energy, which might lead to dislocations.

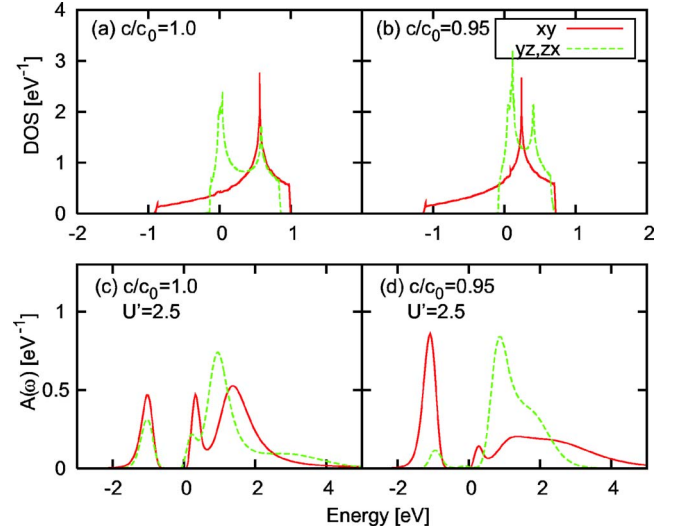


FIG. 6. (Color online) Density of states of the  $t_{2g}$  band of  $\text{Ba}_2\text{VO}_4$  obtained by LDA for (a) atmospheric pressure and (b) uniaxial pressure in the  $c$  direction ( $c/c_0=0.95$ ). (c) and (d) are LDA+DMFT spectral function for (a) and (b), respectively, with  $U'=2.5$  eV.

#### V. CONCLUSION AND DISCUSSION

We found  $\text{Sr}_2\text{VO}_4$  to be an interesting candidate for an orbital switch, triggered by applying high uniaxial pressure. When the  $c$  axis is elongated, only the  $d_{yz/yx}$  bands are occupied,  $\text{Sr}_2\text{VO}_4$  becomes more metallic, and a ferromagnetic instability is to be expected.

On the other hand, when the  $c$  axis is compressed, the system will be more insulating.  $\text{Sr}_2\text{VO}_4$  is then essentially a two-dimensional half-filled single-orbital system, and antiferromagnetic spin fluctuation should dominate. Applying uniaxial pressure in the  $c$  direction, we hence predict  $\text{Sr}_2\text{VO}_4$  to be a  $d^1$  analog of  $d^9$  cuprates, for the effective one-band Hubbard model.

We also study the effect of chemical pressure by substituting Sr by Ba, and find that a  $d^1$  analog of cuprates can be realized more easily by growing  $\text{Ba}_2\text{VO}_4$  on a substrate with lattice constant of 4.1–4.2 Å. If the Hubbard model is the fundamental microscopic model for superconductivity in cuprates, unconventional superconductivity should also be found in  $\text{Sr}_2\text{VO}_4$  or  $\text{Ba}_2\text{VO}_4$  under uniaxial pressure.

#### ACKNOWLEDGMENTS

We thank J. Akimitsu, O. K. Andersen, H. Aoki, H.-U. Habermeier, M. Imada, Y. Imai, K. Kawashima, G. Khaliullin, I. Solovyev, and Y.-F. Yang for fruitful discussions and the Alexander von Humboldt foundation (R.A.) and the Emmy Noether program of the Deutsche Forschungsgemeinschaft (K.H.) for financial support. Numerical calculations were done at the Supercomputer Center, Institute for Solid State Physics, University of Tokyo.

\*Deceased.

- <sup>1</sup>J. G. Bednorz and K. A. Müller, Z. Phys. B: Condens. Matter **64**, 189 (1986).
- <sup>2</sup>P. Hohenberg and W. Kohn, Phys. Rev. **136**, B864 (1964); W. Kohn and L. J. Sham, *ibid.* **140**, A1133 (1965).
- <sup>3</sup>See, e.g., *Strong Coulomb Correlations in Electronic Structure Calculations: Beyond the Local Density Approximation*, edited by V. I. Anisimov (G & B Science, Amsterdam, 1999).
- <sup>4</sup>V. I. Anisimov, A. I. Poteryaev, M. A. Korotin, A. O. Anokhin, and G. Kotliar, J. Phys.: Condens. Matter **9**, 7359 (1997); A. I. Lichtenstein and M. I. Katsnelson, Phys. Rev. B **57**, 6884 (1998).
- <sup>5</sup>K. Held, I. A. Nekrasov, G. Keller, V. Eyert, N. Blümer, A. K. McMahan, R. T. Scalettar, Th. Pruschke, V. I. Anisimov, and D. Vollhardt, Phys. Status Solidi B **243**, 2599 (2006); K. Held, arXiv:cond-mat/0511293 (unpublished); G. Kotliar, S. Y. Savrasov, K. Haule, V. S. Oudovenko, O. Parcollet, and C. A. Marianetti, Rev. Mod. Phys. **78**, 865 (2006).
- <sup>6</sup>A. P. Mackenzie and Y. Maeno, Rev. Mod. Phys. **75**, 657 (2003), and references therein.
- <sup>7</sup>J. Matsuno, Y. Okimoto, M. Kawasaki, and Y. Tokura, Appl. Phys. Lett. **82**, 194 (2003); Phys. Rev. Lett. **95**, 176404 (2005).
- <sup>8</sup>W. E. Pickett, D. Singh, D. A. Papanconstantopoulos, H. Krakauer, M. Cyrot, and F. Cyrot-Lackmann, Physica C **162-164**, 1433 (1989).
- <sup>9</sup>M. J. Rey, Ph. Dehaudt, J. C. Joubert, B. Lambert-Andron, M. Cyrot, and F. Cyrot-Lackmann, J. Solid State Chem. **86**, 101 (1990); A. Nozaki, H. Yoshikawa, T. Wada, H. Yamauchi, and S. Tanaka, Phys. Rev. B **43**, 181 (1991); V. Ginnakopoulou, P. Odier, J. M. Bassat, and J. P. Loup, Solid State Commun. **93**, 579 (1995).
- <sup>10</sup>Y. Imai, I. Solovyev, and M. Imada, Phys. Rev. Lett. **95**, 176405 (2005); Y. Imai and M. Imada, J. Phys. Soc. Jpn. **75**, 094713 (2006).
- <sup>11</sup>H. Weng, Y. Kawazoe, X. Wan, and J. Dong, Phys. Rev. B **74**, 205112 (2006).
- <sup>12</sup>In fact, the LDA+DMFT method has been extensively applied to study correlation-induced orbital charge transfers; see, e.g., A. Liebsch and A. Lichtenstein, Phys. Rev. Lett. **84**, 1591 (2000); K. Held, G. Keller, V. Eyert, D. Vollhardt, and V. I. Anisimov, *ibid.* **86**, 5345 (2001); G. Keller, K. Held, V. Eyert, D. Vollhardt, and V. I. Anisimov, Phys. Rev. B **70**, 205116 (2004); E. Pavarini, S. Biermann, A. Poteryaev, A. I. Lichtenstein, A. Georges, and O. K. Andersen, Phys. Rev. Lett. **92**, 176403 (2004); F. Lechermann, S. Biermann, and A. Georges, *ibid.* **94**, 166402 (2005); H. Ishida, M. D. Johannes, and A. Liebsch, *ibid.* **94**, 196401 (2005); A. Yamasaki, M. Feldbacher, Y. F. Yang, O. K. Andersen, and K. Held, *ibid.* **96**, 166401 (2006).
- <sup>13</sup>J. Yamauchi, M. Tsukada, S. Watanabe, and O. Sugino, Phys. Rev. B **54**, 5586 (1996).
- <sup>14</sup>J. P. Perdew, K. Burke, and Y. Wang, Phys. Rev. B **54**, 16533 (1996).
- <sup>15</sup>D. Vanderbilt, Phys. Rev. B **41**, 7892 (1990).
- <sup>16</sup>K. Laasonen, A. Pasquarello, R. Car, C. Lee, and D. Vanderbilt, Phys. Rev. B **47**, 10142 (1993).
- <sup>17</sup>Because of the large radius of the Sr ion, a significant tilting of the oxygen octahedra is not to be expected.
- <sup>18</sup>O. K. Andersen, Phys. Rev. B **12**, 3060 (1975); O. K. Andersen and O. Jepsen, Phys. Rev. Lett. **53**, 2571 (1984).
- <sup>19</sup>O. K. Andersen and T. Saha-Dasgupta, Phys. Rev. B **62**, R16219 (2000), and references therein.
- <sup>20</sup>The difference can be explained by different support points for linearization and/or *N*-ization [I. Solovyev (private communication)].
- <sup>21</sup>J. E. Hirsch and R. M. Fye, Phys. Rev. Lett. **56**, 2521 (1986).
- <sup>22</sup>A. Sekiyama, H. Fujiwara, S. Imada, S. Suga, H. Eisaki, S. I. Uchida, K. Takegahara, H. Harima, Y. Saitoh, I. A. Nekrasov, G. Keller, D. E. Kondakov, A. V. Kozhevnikov, Th. Pruschke, K. Held, D. Vollhardt, and V. I. Anisimov, Phys. Rev. Lett. **93**, 156402 (2004).
- <sup>23</sup>T. Momoi and K. Kubo, Phys. Rev. B **58**, R567 (1998).
- <sup>24</sup>K. Held and D. Vollhardt, Eur. Phys. J. B **5**, 473 (1998).
- <sup>25</sup>For cluster extension of DMFT see, e.g., T. Maier, M. Jarrell, T. Pruschke, and M. H. Hettler, Rev. Mod. Phys. **77**, 1027 (2005).
- <sup>26</sup>M. S. Hybertsen, E. B. Stechel, M. Schluter, and D. R. Jennison, Phys. Rev. B **41**, 11068 (1990).